MG53 E3 Ligase–Dead Mutant Protects Diabetic Hearts From Acute Ischemic/Reperfusion Injury and Ameliorates Diet-Induced Cardiometabolic Damage

Han Feng,[1] Hao Shen,[1] Matthew J. Robeson,[2] Yue-Han Wu,[1] Hong-Kun Wu,[1] Geng-Jia Chen,[1] Shuo Zhang,[1] Peng Xie,[1] Li Jin,[1] Yanyun He,[1] Yingfan Wang,[1] Fengxiang Lv,[1] Xinli Hu,[1,3] Yan Zhang,[1,4] and Rui-Ping Xiao[1,3,5,6]

Diabetes 2022;71:298–314 | https://doi.org/10.2337/db21-0322

Cardiometabolic diseases, including diabetes and its cardiovascular complications, are the global leading causes of death, highlighting a major unmet medical need. Over the past decade, mitsugumin 53 (MG53), also called TRIM72, has emerged as a powerful agent for myocardial membrane repair and cardioprotection, but its therapeutic value is complicated by its E3 ligase activity, which mediates metabolic disorders. Here, we show that an E3 ligase–dead mutant, MG53-C14A, retains its cardioprotective function without causing metabolic adverse effects. When administered in normal animals, both the recombinant human wild-type MG53 protein (rhMG53-WT) and its E3 ligase–dead mutant (rhMG53-C14A) protected the heart equally from myocardial infarction and ischemia/reperfusion (I/R) injury. However, in diabetic *db/db* mice, rhMG53-WT treatment markedly aggravated hyperglycemia, cardiac I/R injury, and mortality, whereas acute and chronic treatment with rhMG53-C14A still effectively ameliorated I/R-induced myocardial injury and mortality or diabetic cardiomyopathy, respectively, without metabolic adverse effects. Furthermore, knock-in of MG53-C14A protected the mice from high-fat diet–induced metabolic disorders and cardiac damage. Thus, the E3 ligase–dead mutant MG53-C14A not only protects the heart from acute myocardial injury but also counteracts metabolic stress, providing a potentially important therapy for the treatment of acute myocardial injury in metabolic disorders, including diabetes and obesity.

Cardiometabolic disorders, like diabetes, ischemia heart disease, and heart failure, are the major causes of death around the world (1,2). Patients with diabetes experience worse outcomes when combined with cardiovascular comorbidities, including acute myocardial infarction, coronary angioplasty, cardiac bypass surgery, and heart failure (3–7). Hyperglycemia and diabetes diminish intrinsic cardiac protective effects for both ischemic preconditioning (IPC) and postconditioning in rodents (8–12) and exacerbate ischemia/reperfusion (I/R)–induced myocardial injury in humans and animals (13–15). Thus, glycemic control is beneficial in individuals with diabetes with acute myocardial injury and chronic heart failure (7,16).

We and others have previously demonstrated that endogenous mitsugumin 53 (MG53), also called TRIM72, plays an essential role in cardioprotection mediated by IPC and postconditioning (17,18). While MG53 deficiency exacerbates I/R-induced myocardial damage, overexpression or systemic delivery of recombinant human MG53 protein (rhMG53) mitigates acute myocardial infarction–

[1]State Key Laboratory of Membrane Biology, Institute of Molecular Medicine, College of Future Technology, Peking University, Beijing, China
[2]Department of Biomedical Engineering, Georgia Institute of Technology and Emory University, Atlanta, GA
[3]Beijing City Key Laboratory of Cardiometabolic Molecular Medicine, Peking University, Beijing, China
[4]Key Laboratory of Molecular Cardiovascular Sciences, Institute of Cardiovascular Sciences, Ministry of Education, School of Basic Medical Sciences, Peking University Health Science Center, Beijing, China
[5]Peking-Tsinghua Center for Life Sciences, Peking University, Beijing, China
[6]Peking University–Nanjing Joint Institute of Translational Medicine, Nanjing, China

Corresponding authors: Rui-Ping Xiao, xiaor@pku.edu.cn, and Yan Zhang, zhangyan9876@pku.edu.cn

Received 18 April 2021 and accepted 14 November 2021

This article contains supplementary material online at https://doi.org/10.2337/figshare.17026526.

H.F. and H.S. contributed equally to this work.

and I/R-induced heart injury and improves the function of failing hearts in mice, rats, and swine (19,20). Thus, rhMG53 may serve as an effective therapy to treat acute myocardial injury.

However, MG53 is a double-edged sword for human diseases. Upregulation of MG53 impairs insulin receptor (IR) signaling, leading to insulin resistance and hyperglycemia, which may compromise the efficacy of MG53-mediated cardioprotection and raise safety concerns in clinical applications. Previous work has shown that transgenic overexpression of MG53 triggers metabolic syndrome characterized by obesity, hyperglycemia, dyslipidemia, and hypertension, whereas MG53 deficiency relieves high-fat diet (HFD)–induced insulin resistance, dysregulation of glucose and lipid metabolism, and obesity in mice (21). Mechanistically, intracellular MG53 acts as a ubiquitin E3 ligase, targeting IR and its interacting protein IR substrate 1 (IRS1) for ubiquitination-dependent degradation in striated muscle (21,22). In addition to its intracellular action, MG53 is secreted under metabolic or oxidative stress conditions, such as high glucose or high insulin or increased reactive oxygen (O_2) species production (19,23,24). Elevated circulating MG53 suppresses insulin signaling in multiple organs, including heart, skeletal muscle, liver, and adipose tissue in nondiabetic mice. However, neutralizing blood MG53 with anti-MG53 antibodies ameliorates hyperglycemia and insulin intolerance in *db/db* mice (23), suggesting that administration of MG53 may trigger systemic insulin resistance and aggravate diabetes and its cardiovascular complications. Therefore, it is pivotal to determine whether systemic delivery of rhMG53 is beneficial or detrimental to individuals with diabetes with cardiovascular complications.

Because the undesired metabolic effects of MG53 are mainly caused by its E3 ligase activity, we investigated whether the MG53 E3 ligase–dead mutant C14A (21,22,24) could overcome the metabolic adverse effects of MG53 systemic treatment while retaining its cardioprotective function. Using wild-type (WT) rhMG53 (rhMG53-WT) or C14A mutant (rhMG53-C14A) treatment in conjunction with MG53-C14A knock-in mice, we show that rhMG53-C14A is as potent as rhMG53-WT in protecting the heart against I/R injury in nondiabetic mice in vivo and in cultured cardiac myocytes. In diabetic mice, however, rhMG53-WT treatment worsens hyperglycemia and I/R-induced myocardial injury and mortality. In sharp contrast, rhMG53-C14A protects the heart from I/R injury without disrupting metabolic homeostasis. Furthermore, sustained expression of MG53-C14A in the knock-in mice not only preserved IPC cardioprotection, but also markedly diminished HFD-induced insulin resistance and a cluster of metabolic disorders, including hyperglycemia, dyslipidemia, obesity, and cardiac dysfunction. These findings define MG53-C14A as a promising therapy to treat acute myocardial injury and perhaps some chronic cardiometabolic disorders.

RESEARCH DESIGN AND METHODS

Animal Studies

All animal experiments were performed in accordance with the guidelines of the Institutional Animal Care and Use Committee of Peking University and conformed to the Guide for the Care and Use of Laboratory Animals.

db/db and *db/*$^{+}$ mice were purchased from Beijing Vital River Animal Laboratory (Beijing, China). *KKAy* and *KK* mice were purchased from Beijing HFK Bioscience (Beijing, China). The MG53-C14A knock-in founder with chimera background of C57BL/6 and 129/SvJ was established by homologous recombination and blastocyst injection. Homozygous MG53-C14A knock-in mice with C57BL/6 background (MG53-C14A [ki/ki] mice) were prepared by chimera backcross over 7 generations. Generation of *Mg53*$^{-/-}$ mice and dietary intervention were described previously (21). Genotyping was performed by PCR before initiation of the experiments and after the euthanization of the animals. Both male and female mice were used in this study. HFD (cat. no. D12492; Research Diets, Inc., New Brunswick, NJ) or standard chow (Academy of Military Medical Sciences, Beijing, China) were started from 4 weeks of age. Experiments including myocardial I/R, heart Langendorff perfusion, recombinant protein injection, and adenovirus infection were performed in adult mice at 10 weeks of age, if not noted.

Mouse In Vivo Myocardial I/R Model

For animal models of myocardial ischemia and the assessment of cardiac injury, we referred to the published guidelines (25,26). Adult male mice were anesthetized under isoflurane anesthesia (0.8% to 1.2% in 100% O_2) and ventilated via a tracheostomy on a Harvard rodent respirator. A midline sternotomy was performed, and a reversible coronary artery snare occluder was placed around the left anterior descending coronary artery. Myocardial I/R was performed by tightening the snare for 30 min and then loosening it for 24 h (for infarct size measurement). At the end point, hearts were excised and stained with 2,3,5-tetraphenyltetrazolium chloride (Chemical Abstracts Service [CAS] no. 298-96-4; Sigma-Aldrich) to indicate infarct area using standard techniques (27). Blood samples were collected and centrifuged for 10 min at 3,000 rpm to collect serum for the measurement of lactate dehydrogenase (LDH) (cat. no. MAK066; Sigma-Aldrich), creatine kinase (CK) (cat. no. ML037292; Shanghai Enzyme-linked Biotechnology), and cardiac troponin T (cTnT) (cat. no. ML037723; Shanghai Enzyme-linked Biotechnology).

Isolated Mouse Heart Langendorff Perfusion

Adult male mice were harvested by i.p. injection of pentobarbital (70 mg/kg), followed by removal of the heart, which was then perfused on a Langendorff apparatus at

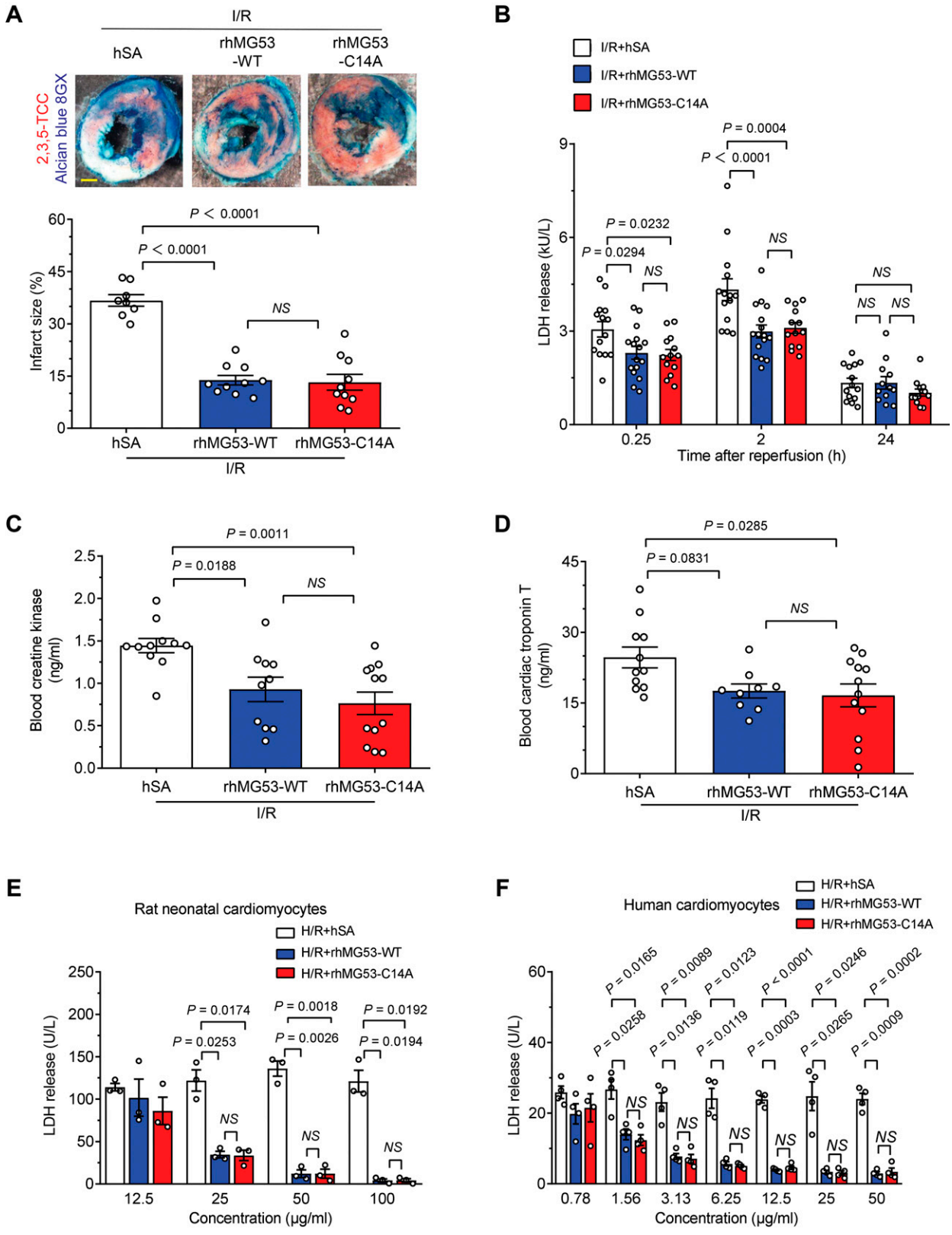

Figure 1—rhMG53-C14A preserves its protective effect on nondiabetic mouse hearts and cultured cardiomyocytes. *A–D*: Representative images and statistical data of myocardial infarct size (n = 8, 10, and 10 for I/R + hSA, I/R + rhMG53-WT, and I/R + rhMG53-C14A, respectively, from nondiabetic *db*/$^{+}$ mice; the order of the groups is the same in all the panels) (*A*), serum LDH levels (n = 14, 16, and 13, respectively) (*B*), blood CK (n = 11, 10, and 12, respectively) (*C*), and cTnT levels (n = 11, 9, and 12, respectively) (*D*) induced in vivo by I/R in combination with 1 mg/kg (i.p.) hSA, rhMG53-WT, or rhMG53-C14A treatment. Scale bar is 1 mm. *E* and *F*: Levels of LDH release from

constant pressure. The hearts were perfused with a modified Krebs-Henseleit solution (118.5 mmol/L sodium chloride, 25.0 mmol/L sodium bicarbonate, 4.7 mmol/L potassium chloride, 1.2 mmol/L magnesium sulfate, 1.2 mmol/L monopotassium phosphate, 11 mmol/L glucose, and 2.5 mmol/L calcium chloride) continuously gassed with 95% O_2/5% carbon dioxide (CO_2) (pH 7.4) and warmed by a heating bath/circulator at 37°C (range 36.5–37.5°C). Global ischemia was induced by cessation of perfusion for 30 min followed by reperfusion. IPC was achieved by two cycles of 5 min of ischemia followed by 5 min of reperfusion before a more sustained I/R that caused myocardial infarction was achieved. The effluent from the perfused heart was measured for LDH. After reperfusion for 120 min, hearts were removed from the apparatus and stained with 2,3,5-tetraphenyltetrazolium chloride to indicate infarct area using standard techniques (27).

Cardiomyocyte Culture and Hypoxia/Reoxygenation

Human cardiomyocytes were purchased from Promocell (cat. no. C-12810). Isolation and culture of neonatal rat ventricular myocytes were described previously (17). Human serum albumin (hSA) (CAS no. 70024-90-7; Heowns Biochem Technologies), rhMG53-WT (cat. no. tp810010), and rhMG53-C14A (cat. no. tp800125dm) were purchased from OriGene Technologies (Rockville, MD). For exogenous protein pretreatment, hSA, rhMG53-WT, and rhMG53-C14A were incubated with cardiomyocytes before hypoxia/reoxygenation (H/R).

The H/R experiments were performed as previously described (17). In brief, cells were first cultured in RPMI 1640 (cat. no. A1049101; Gibco)/5% FBS (cat. no. 10091155; Gibco) with exogenous protein pretreatment as described. Then, the medium was changed to serum-free RPMI 1640 saturated with 95% nitrogen/5% CO_2, and cells were placed in a 37°C airtight box saturated with 95% nitrogen/5% CO_2 for 30 min. O_2 concentrations were <0.1% (Ohmeda O_2 monitor type 5120). Finally, the medium was changed to serum-free RPMI 1640, and cells were placed in a 37°C 5% CO_2 incubator for 2 h before analysis.

Recombinant Protein Injection

hSA, rhMG53-WT, and rhMG53-C14A were prepared as 2–5 mg/mL in 0.01 mol/L PBS and then injected i.p. as 1 mg/kg body weight into mice as described in each experiment.

Metabolic Measurements

For glucose tolerance tests, mice fasted overnight (16 h) and were then injected i.p. with D-glucose as 2 g/kg body weight (CAS no. 50-99-7; Sigma-Aldrich). For insulin tolerance tests, mice were randomly fed and injected i.p. with bovine insulin as 0.75 units/kg body weight (cat. no. 11070-73-8; Sigma-Aldrich). We collected blood from a tail vein before injection and at different time points after injection. Glucose was measured with an AccuCheck blood glucose meter (Roche Diagnostics, Inc.). Serum nonesterified fatty acid, triglyceride, and cholesterol concentrations were spectrophotometrically assayed with commercial kits (cat. nos. 294-63601, 290-63701, and 294-65801, respectively; FUJIFILM Wako Diagnostics).

For metabolic rate analysis, mice were housed individually under a 12-h light/dark cycle. A comprehensive animal metabolic monitoring system (Comprehensive Lab Animal Monitoring System; Columbus Instruments) was used to evaluate VO_2 and VCO_2 continuously over a 72-h period. Energy expenditure was calculated using the following formula: energy expenditure = $(3.815 + 1.232\ VO_2/VCO_2) \times VO_2$. Food consumption was also recorded using the Comprehensive Lab Animal Monitoring System.

Echocardiography

Adult male mice were anesthetized with isoflurane (0.8% to 1.2% in 100% O_2), and echocardiography assessment was performed using a VEVO-2100 machine (FUJIFILM VisualSonics).

Establishment of Human MG53 ELISA Kit

For anti-MG53 antibody panning, the extracellular domains of human and murine MG53 were labeled with a His-Avitag and biotinylated by BirA ligase or labeled with His-tag. These proteins were used as antigens in the panning experiments with a human nonimmune single-chain fragment of variable domain (scFv) (variable heavy chain + linker + varible light chain) antibody library (1.1×10^{10}), which was constructed from peripheral blood mononuclear cells from 93 healthy donors. Briefly, the antigens were initially captured on streptavidin-conjugated magnetic M-280 Dynabeads (Thermo Fisher Scientific) or Nunc-Immuno Tubes and then incubated with 1×10^{13} phage scFv particles prepared from the library. Unbound particles were washed off, and bound particles were then eluted and amplified for the next round of panning. For each panning, seeking to obtain high-affinity antibodies, we optimized the amount of antigen captured and applied extensive washing six times by PBS. In addition, to recover high-affinity binders from the magnetic beads and increase the diversity of phage scFv

either cultured rat neonatal cardiomyocytes (data are representative of three independent experiments) (*E*) or human cardiomyocytes (data are representative of four independent experiments) (*F*) subjected to H/R with hSA, rhMG53-WT, or rhMG53-C14A treatment at different concentrations. All data are presented as mean ± SEM. Statistical analysis was conducted by one-way ANOVA with Tukey multiple comparisons test (*A*, *C*, and *D*) or two-way ANOVA with Tukey multiple comparisons test (*B*, *E*, and *F*). NS, not significant.

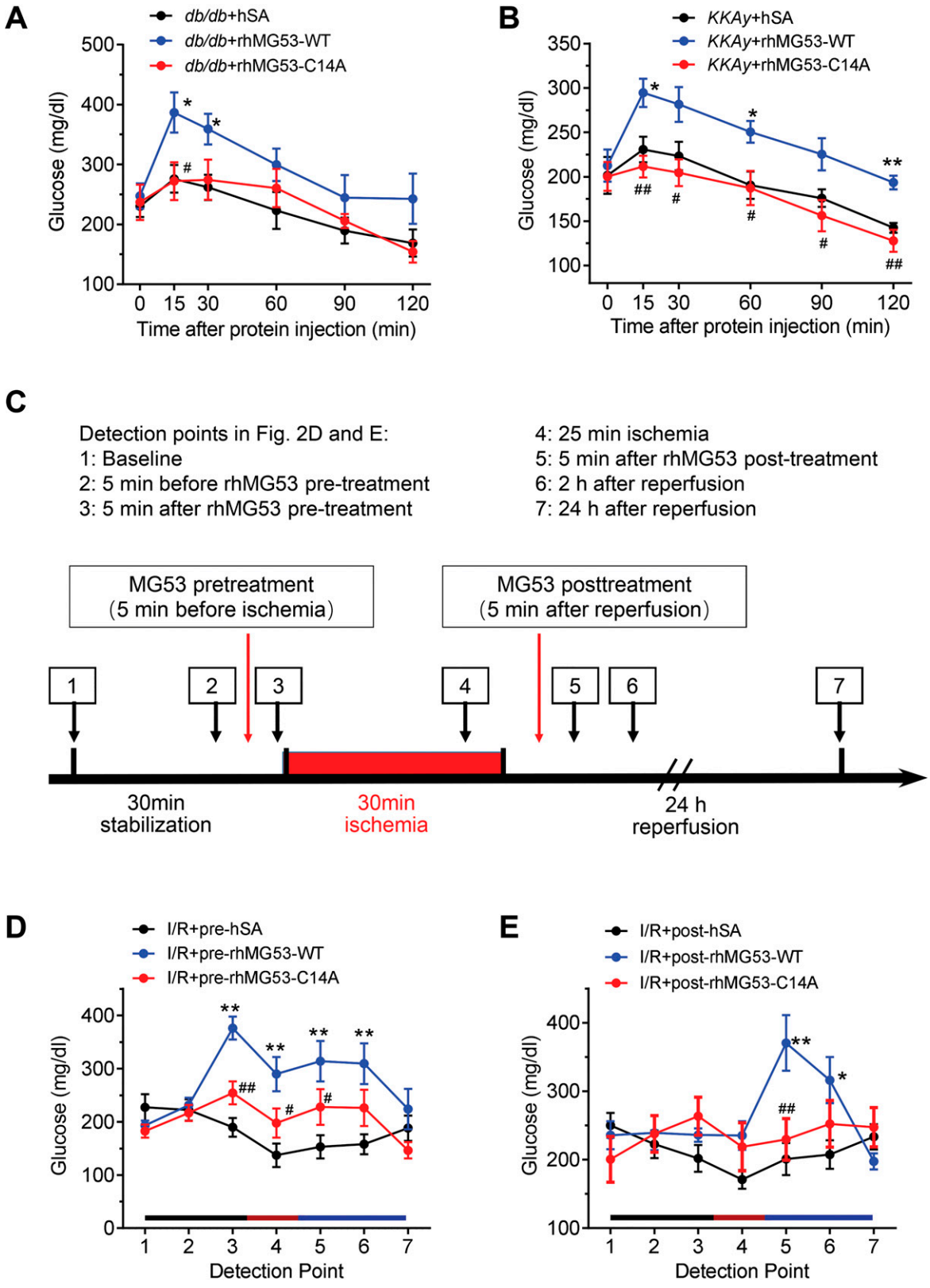

Figure 2—rhMG53-WT, but not rhMG53-C14A, induces hyperglycemia in diabetic mice. *A* and *B*: Alterations of blood glucose in diabetic *db/db* mice ($n = 8$ *db/db* + hSA, $n = 6$ *db/db* + rhMG53-WT, and $n = 6$ *db/db* + rhMG53-C14A) (*A*) and *KKAy* mice ($n = 7$ *KKAy* + hSA, $n = 6$ *KKAy* + rhMG53-WT, and $n = 8$ *KKAy* + rhMG53-C14A) (*B*) injected with 1 mg/kg (i.p.) hSA, rhMG53-WT, or rhMG53-C14A. *C*: Experimental procedures for blood glucose monitoring in panels *D* and *E*. Pretreatment and posttreatment were 5 min before and after cardiac ischemia, respectively. Blood glucose levels were determined at the time points indicated by the arrows. *D* and *E*: Responses to blood

recovered, both phage particles from the conventional basic triethanolamine elution and phage particles still captured on the M-280 Dynabeads or Nunc-Immuno Tubes after the elution were retained for further analysis. A total of ~1,300 single clones were randomly picked and rescued for binding analysis in the bacterial culture supernatant. These clones were then screened for binding to MG53 by ELISA. Clones selected out were produced as purified phage scFv particles and converted into an scFv-hFc format and then reanalyzed for binding ability by surface plasmon resonance or ELISA (28). The ELISA kit was used for serum MG53 measurement.

Adenovirus Establishment and Infection

rhMG53-WT and MG53-C14A mutant were fused with a tissue plasminogen activator (tPA) signal peptide at the N-terminus and cloned into pCDNA3.1. Adenovirus expressing tPA-rhMG53-WT or tPA-rhMG53-C14A was established by BAC Biological Technology (Beijing, China). For adenovirus infection in mice, 100 μL of high-titer adenovirus (1×10^8 colony-forming units/mL) was diluted in saline and then injected i.v. as 5×10^5 colony-forming units/kg body weight into mice.

The sequence of the tPA signal peptide was as follows: 5′-ATGGATGCAATGAAGAGAGGGCTCTGCTGTGTGCTGC-TGCTGTGTGGAGCAGTCTTCGTTTCGCCC-3′.

Histological Analysis

The tissues for histological analysis were fixed overnight in 4% paraformaldehyde (pH 7.4), embedded in paraffin, serially sectioned at 5 μm, and stained with hematoxylin and eosin. Oil red O staining was performed with a commercial kit (cat. no. BA-4081; Baso Diagnostic, Inc.). Images were captured by the EVOS FL Auto microscope (cat. no. AMAFD1000; Thermo Fisher Scientific, Waltham, MA).

Western Blots

Tissues or cells were lysed in lysis buffer A (30 mmol/L HEPES [pH 7.6], 100 mmol/L sodium chloride, 0.5% Nonidet P-40, and protease inhibitor mixture) on ice for 10 min, and the lysates were centrifuged at 13,000 rpm for 10 min. The Western blot assays were performed as described previously (17). All proteins were analyzed with specific antibodies. The anti-MG53 monoclonal antibody (final concentration 0.5 μg/mL) was customized (23). GAPDH antibody (cat. no. BE0034-100 (1:10,000) and β-actin antibody (cat. no. BE0037-100) (1:10,000) were purchased from Bioeasy Technology. The anti-IR antibody (cat. no. ab203278) (1:1,000) was from Abcam. The anti-IRS1 antibody (cat. no. 2390S) (1:1,000), anti–phospho-Akt antibody (phosphorylation at Ser473) (cat. no. 4060) (1:1,000), anti–total Akt antibody (cat. no. 9272) (1:1,000), and ubiquitin antibody (cat. no. 3936) (1:1,000) were from Cell Signaling Technology. Myc-tag antibody (cat. no. M5546) (1:5,000) was from Sigma-Aldrich.

Ubiquitination Assay

To assay in vivo ubiquitination, skeletal muscles were ground into powder in liquid nitrogen, lysed with radioimmunoprecipitation assay buffer mentioned above for 1 h at 4°C, and then centrifuged at 13,000 rpm for 10 min. Protein A agarose beads were incubated with indicated antibody for 8 h at 4°C, followed by incubation with a total of 700 mg lysate for another 3 h at 4°C. The immunoprecipitated beads were extensively washed in radioimmunoprecipitation assay buffer, eluted with 2× SDS sample buffer, and analyzed by Western blots.

Statistical Analysis

Statistical parameters and significance are reported in figures and figure legends. Data are expressed as mean ± SEM. Statistical analysis was performed with GraphPad Prism version 8.01. Data sets were tested for normality of distribution with the Kolmogorov-Smirnov test. Comparisons among multiple groups were assessed by one-way ANOVA with Tukey multiple comparisons test. Comparisons between two groups or among multiple groups at multiple time points were assessed by two-way ANOVA with Sidak or Tukey multiple comparisons test. Survival curves were assessed by the log-rank (Mantel-Cox) test. No statistical method was used to predetermine sample size.

Data and Resource Availability

All the data sets and resources generated and/or analyzed during the current study are available from the corresponding author upon reasonable request.

RESULTS

Both rhMG53-C14A and rhMG53-WT Effectively Protect the Heart From I/R Injury in Nondiabetic Mice and Cultured Cardiomyocytes

To compare the efficacy of rhMG53-WT and rhMG53-C14A, we treated *db*/$^+$ mice with each recombinant protein (1 mg/kg i.p.) separately and assayed the serum MG53 levels by a customized ELISA kit. Injection with recombinant hSA was used as a control. Both proteins

glucose levels in diabetic *db*/*db* mice subjected to I/R in vivo with different regimens of i.p. hSA, rhMG53-WT, or rhMG53-C14A treatment. Pretreatment, injected before ischemia (n = 9 I/R + pre-hSA, n = 17 I/R + pre-rhMG53-WT, and n = 14 I/R + pre-rhMG53-C14A) (*D*), and posttreatment, injected after ischemia (n = 8 I/R + post-hSA, n = 8 I/R + post-rhMG53-WT, and n = 9 I/R + post-rhMG53-C14A) (*E*). All data are presented as mean ± SEM. Statistical analysis was conducted by two-way ANOVA with Tukey multiple comparisons test (*A*, *B*, *D*, and *E*). *A* and *B*: *$P < 0.05$, **$P < 0.01$ for *db*/*db* (*KKAy*) + rhMG53-WT vs. *db*/*db* (*KKAy*) + hSA; #$P < 0.05$, ##$P < 0.01$ for *db*/*db* (*KKAy*) + rhMG53-C14A vs. *db*/*db* (*KKAy*) + rhMG53-WT. *D* and *E*: *$P < 0.05$, **$P < 0.01$ for I/R + pre- and post-rhMG53-WT vs. I/R + pre- and post-hSA; #$P < 0.05$, ##$P < 0.01$ for I/R + pre- and post-rhMG53-C14A vs. I/R + pre- and post-rhMG53-WT.

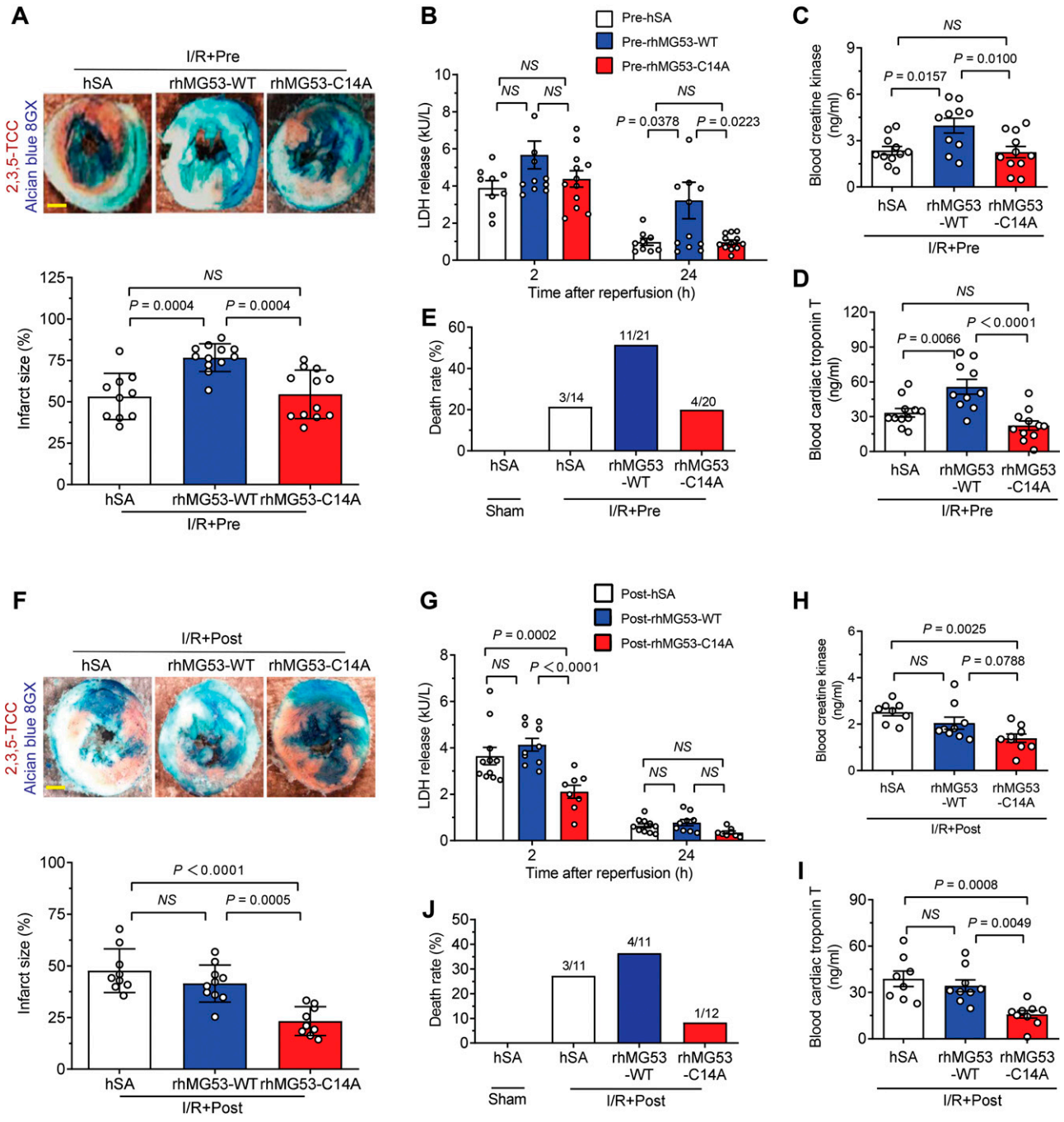

Figure 3—rhMG53-C14A is beneficial, but rhMG53-WT is detrimental, for diabetic hearts subjected to I/R injury. *A–E*: Representative images and statistical data of myocardial infarct size (n = 10, 12, and 12) (*A*), serum LDH levels (n = 9, 12, and 12) (*B*), blood CK (n = 11, 10, and 11) (C), cTnT levels (n = 11, 10, and 11) (D), and mortality (n = 14, 21, and 20) (E) in diabetic *db/db* mice subjected to I/R in vivo with hSA, rhMG53-WT, or rhMG53-C14A pretreatment, respectively. *F–J*: Representative photographs and statistical data of myocardial infarct size (n = 9, 10, and 9) (*F*), serum LDH levels (n = 11, 10, and 8) (G), blood CK (n = 8, 9, and 9) (*H*), cTnT levels (n = 8, 9, and 9) (*I*), and mortality (n = 11, 11, and 12) (*J*) in diabetic *db/db* mice subjected to I/R in vivo with hSA, rhMG53-WT, or rhMG53-C14A posttreatment, respectively. Scale bar is 1 mm. All data are presented as mean ± SEM. Statistical analysis was conducted by one-way ANOVA with Tukey multiple comparisons test (*A*, *C*, *D*, *F*, *H*, and *I*) or two-way ANOVA with Tukey multiple comparisons test (*B* and *G*). NS, not significant.

reached a peak serum concentration of 20.5 μg/mL within 20 min after injection, then gradually reduced to T50 (50% decrease) and T90 (90% decrease) at 30 and 45 min, respectively (Supplementary Fig. 1*A*). There was no difference between diabetic *db/db* mice and the non-diabetic *db/*$^{+}$ controls in terms of the kinetics of MG53 serum concentration (Supplementary Fig. 1*B*). Importantly, compared with the control group, both rhMG53-WT and

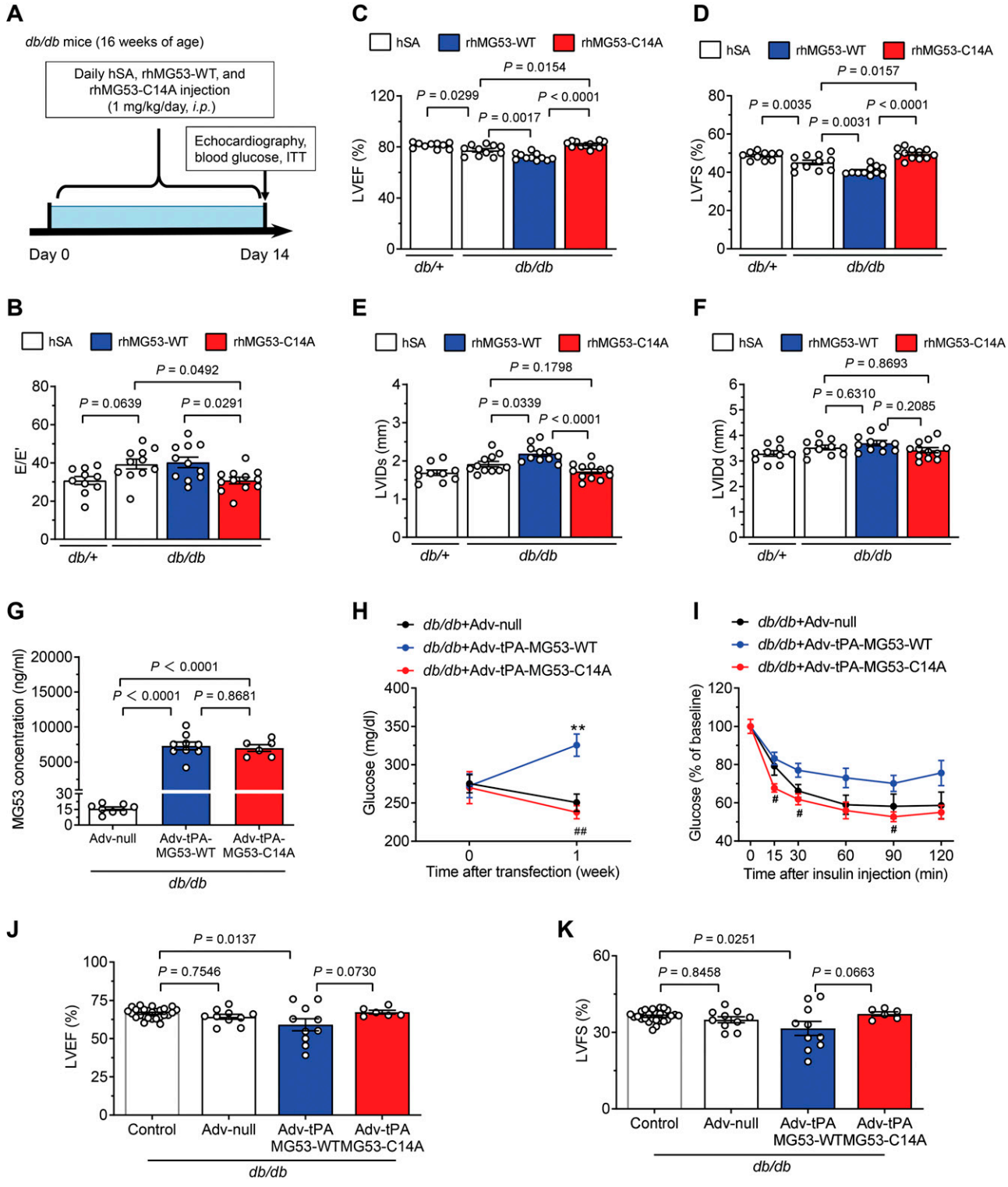

Figure 4—Chronic treatment with rhMG53-C14A is beneficial, but rhMG53-WT is detrimental, to the cardiac function of diabetic hearts. *A*: Experimental procedures for chronic treatment with hSA, rhMG53-WT, and rhMG53-C14A. *B–F*: Statistical results of left ventricular diastolic function (indexed by E/E′) (*B*) and systolic function (indexed by left ventricular ejection fraction [LVEF]) (*C*) and fractional shortening (LVFS) (*D*), and systolic (LVIDs) (*E*) and diastolic left ventricular internal diameter (LVIDd) (*F*) of the diabetic *db/db* mice treated with hSA, rhMG53-WT, or rhMG53-C14A as per the protocol in panel *A*. The *db*/$^{+}$ mice treated with hSA were used as controls (n = 10, 11, 11, and 12, respectively). *G–K*: Circulating MG53 levels (n = 8 *db/db* + control adenovirus [Adv-null], n = 9 *db/db* + Adv–tissue plasminogen activator [tPA]–MG53-WT, and n = 6 *db/db* + Adv-tPA-MG53-C14A; the same group order is shown below) (*G*), blood glucose levels (n = 8, 9, and 6, respectively) (*H*), insulin tolerance tests (ITT) (n = 5, 5, and 6, respectively) (*I*), and cardiac systolic function (n = 10, 10 and 6, respectively) for LVEF (*J*) and LVFS (*K*) in diabetic *db/db* mice 1 week after infection with adenovirus-overexpressing circulating WT (Adv-tPA-

rhMG53-C14A profoundly reduced the infarct size from 36.7% to <14% (Fig. 1*A* and Supplementary Fig. 2*A*) and significantly suppressed I/R-induced myocardial membrane breakage indexed by LDH release at indicated time points after reperfusion (Fig. 1*B*). Moreover, rhMG53-C14A and rhMG53-WT were equally potent in lowering the blood CK and cTnT levels (Fig. 1*C* and *D*). These data indicate that administration of MG53 with C14A mutation exerts a cardioprotective ability comparable to that of MG53-WT in nondiabetic *db*/$^{+}$ mice. rhMG53-WT and rhMG53-C14A also attenuated H/R-induced LDH release in cultured rat neonatal cardiomyocytes in a dose-dependent manner (Fig. 1*E* and Supplementary Fig. 2*C*). More importantly, they indistinguishably promoted the survival of human cardiomyocytes challenged by H/R (Fig. 1*F* and Supplementary Fig. 2*C*), revealing a high therapeutic potential for rhMG53-C14A as well as rhMG53-WT in treating acute injury of human hearts regardless of relatively low endogenous MG53 expression (29).

rhMG53-C14A Is Beneficial But rhMG53-WT Is Detrimental for Diabetic Hearts Subjected to I/R Injury

Previous studies have shown that injection of rhMG53-WT impairs insulin signaling in multiple organs in mice (23). Here we traced blood glucose levels in multiple diabetic models after injection of recombinant proteins. Injection of rhMG53-WT neither changed basal blood glucose in *db*/$^{+}$ or *KK* control mice nor altered systemic glucose tolerance or insulin sensitivity compared with hSA injection in control animals (Supplementary Fig. 3*A–D*). However, in diabetic *db*/*db* and *KKAy* mice, rhMG53-WT triggered an acute increase in blood glucose, which peaked within 15 min and remained high for at least 60 min (Fig. 2*A* and *B*). In contrast, rhMG53-C14A did not affect blood glucose in either *db*/*db* or *KKAy* mice as compared with the corresponding control group (Fig. 2*A* and *B*), suggesting that C14A mutation is likely devoid of MG53-mediated metabolic adverse effects in diabetic mice.

To simulate different clinical scenarios, we treated *db*/*db* mice with 1 mg/kg rhMG53-WT, rhMG53-C14A, or the control protein (hSA) before (pretreatment, designated as pre-rhMG53 or pre-hSA) or after (posttreatment, designated as post-rhMG53 or post-hSA) 30-min ischemia during I/R surgery and monitored blood glucose at the indicated time points (Fig. 2*C* and Supplementary Fig. 2*A* and *B*). While both pre- and post-rhMG53-WT increased blood glucose, the effect of pretreatment persisted much longer than that of post-treatment (Fig. 2*D* and *E*). In contrast, neither pre- nor post-rhMG53-C14A treatment affected blood glucose relative to the control group (pre-hSA and post-hSA, respectively) (Fig. 2*D* and *E*). Thus, rhMG53-WT, but not its C14A mutant, further elevated blood glucose on top of diabetic hyperglycemia.

Notably, pre-rhMG53-WT worsened I/R-induced myocardial injury in *db*/*db* mice, as evidenced by markedly enlarged infarct size, increased LDH release, and elevated blood CK and cTnT levels, whereas pre-rhMG53-C14A did not instigate any of these detrimental effects in these mice (Fig. 3*A–D*). Concomitantly, pre-rhMG53-WT, but not pre-rhMG53-C14A, overtly increased I/R-induced mortality (Fig. 3*E*). Most importantly, post-rhMG53-C14A, but not post-rhMG53-WT, profoundly protected the diabetic mice from I/R-induced myocardial injury and mortality (Fig. 3*F–J*). Taken together, posttreatment with rhMG53-C14A effectively attenuated I/R-induced cardiac injury and decreased death in diabetic mice without causing metabolic adverse effects, whereas pretreatment as well as posttreatment with rhMG53-WT exaggerated cardiac I/R injury and increased mortality.

To evaluate the effect of long-term treatment of the MG53 mutant on diabetic hearts, we treated diabetic *db*/*db* mice (16 weeks of age) with rhMG53-WT, rhMG53-C14A, or hSA for 2 weeks (Fig. 4*A*). Compared with the control group (*db*/$^{+}$ mice treated with hSA), both systolic and diastolic functions of left ventricle were impaired in *db*/*db* mice with hSA treatment, which further deteriorated with rhMG53-WT treatment in the diabetic mice (Fig. 4*B–D*). Importantly, long-term treatment with rhMG53-C14A restored the cardiac function of the diabetic mice (Fig. 4*B–D*), without causing metabolic adverse effects (Supplementary Fig. 4*A* and *B*). Furthermore, treatment with rhMG53-WT, but not rhMG53-C14A, induced the enlargement of left the ventricle in the *db*/*db* mice (Fig. 4*E* and *F*). Thus, long-term treatment with rhMG53-C14A, but not rhMG53-WT, effectively improves cardiac function in diabetic *db*/*db* mice with a good safety profile.

Although the bolus intraperitoneal injection of rhMG53-WT, but not hSA or rhMG53-C14A, triggered an acute and transient increase in blood glucose in the *db*/*db* mice (Fig. 2*A*), daily injection of rhMG53-WT for 2 weeks was not sufficient to alter basal blood glucose or insulin tolerance (Supplementary Fig. 4*A* and *B*). We next investigated the effects of a prolonged and sustained elevation of blood MG53 in diabetic animals using adenoviral gene transfer of hMG53 or its C14A mutant fused with a signal peptide of tissue plasminogen activator (Supplementary Fig. 5*A*) (30,31). Adenoviral gene transfer increased MG53 levels in the liver but not the heart (Supplementary Fig. 5*B*). While adenoviral overexpression of

MG53-WT) or C14A-mutated (Adv-tPA-MG53-C14A) hMG53 or Adv-null. Age-matched diabetic *db*/*db* mice treated with saline solution (n = 26 *db*/*db* controls) served as negative controls in panels *J* and *K*. All data are presented as mean ± SEM. Statistical analysis was conducted by one-way ANOVA with Tukey multiple comparisons test (*B–G*, *J*, and *K*) or two-way ANOVA with Tukey multiple comparisons test (*H* and *I*). *H* and *I*: $^{**}P < 0.01$ for *db*/*db* + Adv-tPA-MG53-WT vs. *db*/*db* + Adv-null; $\#P < 0.05$, $\#\#P < 0.01$ for *db*/*db* + Adv-tPA-MG53-C14A vs. *db*/*db* + Adv-tPA-MG53-WT. NS, not significant.

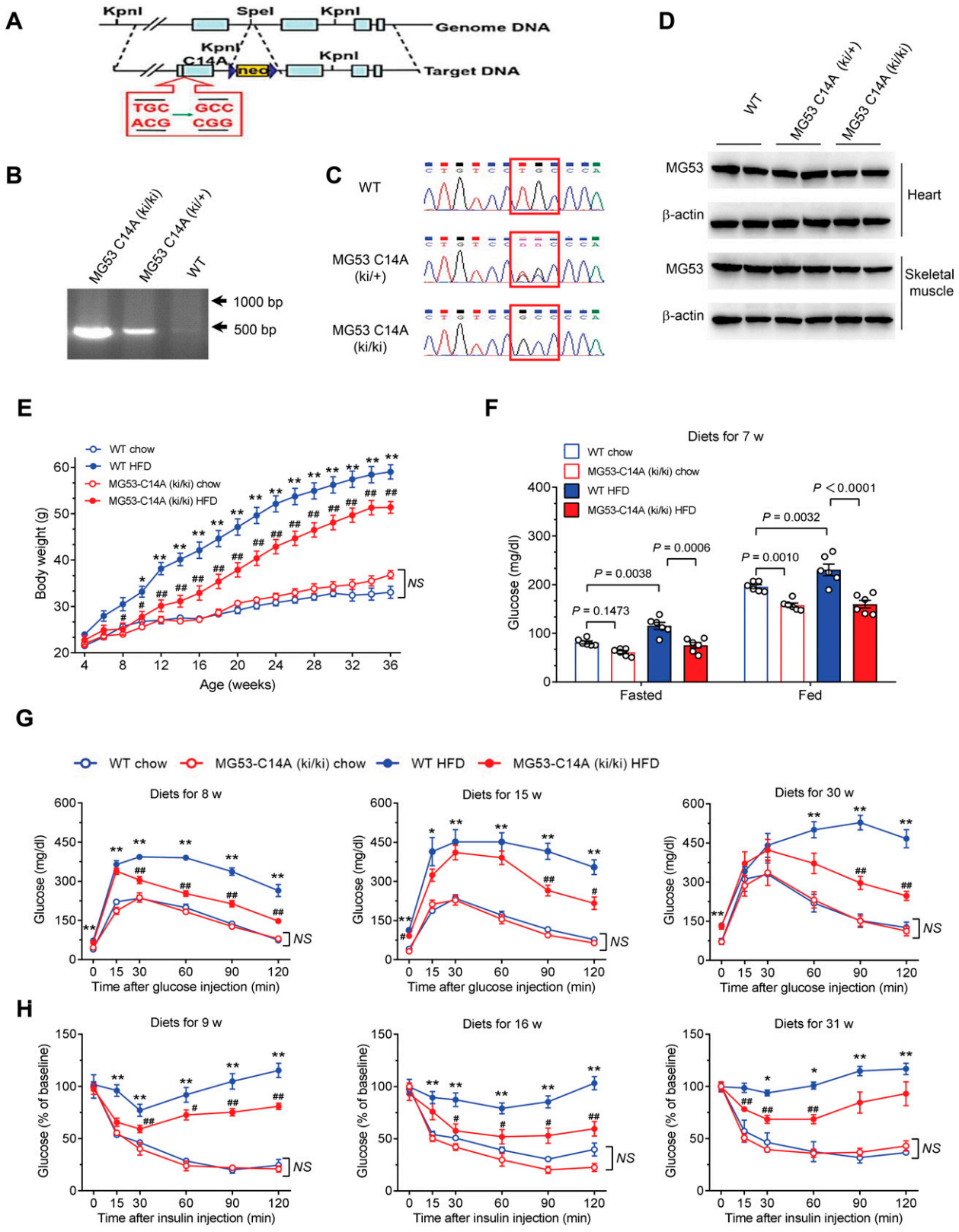

Figure 5—MG53-C14A knock-in mice are resistant to HFD-induced obesity, hyperglycemia, glucose intolerance, and insulin resistance. *A*: Schematic diagram showing the targeting strategy of MG53-C14A knock-in mice. *B* and *C*: Representative genotyping results, including electrophoretogram (*B*) and sequencing (*C*), of WT littermates and heterozygote MG53-C14A (ki/$^{+}$), and homozygote MG53-C14A (ki/ki) mice. *D*: Representative Western blots of MG53 in the heart and skeletal muscle of MG53-C14A (ki/ki) and MG53-C14A (ki/$^{+}$) mice and their WT littermates. β-actin served as a loading control. *E–H*: The metabolic features of homozygous MG53-C14A knock-in (MG53-C14A [ki/ki]) mice and their WT littermates administered chow diet or HFD from 4 weeks of age. For the number of animals used in each

secreted hMG53-WT and its E3 ligase–dead mutant increased blood MG53 and its C14A mutant proteins to a similar level in *db/db* mice 1 week after i.v. injection (Fig. 4*G*), elevated MG53-WT, but not C14A mutant, levels resulted in anabatic blood glucose, impaired blood glucose tolerance, and cardiac dysfunction (Fig. 4*H–K*). In line with the outcomes of the chronic treatment of recombinant proteins, these results with adenoviral gene transfer imply that MG53-C14A is a promising therapeutic strategy for the treatment of diabetes-associated acute myocardial infarction and I/R injury and, equally important, call for caution in the use of rhMG53-WT in the setting of diabetes.

MG53-C14A Knock-in Mice Are Resistant to HFD-Induced Obesity and Metabolic Disorders

Despite the fact that in vivo and in vitro data strongly imply that rhMG53-C14A is a promising therapy for acute myocardial I/R injury in individuals with diabetes, it is unclear whether prolonged use of MG53-C14A is safe and effective in treating chronic cardiometabolic diseases. To address this important question, we generated MG53-C14A knock-in mice (Fig. 5*A–C*). The expression levels of MG53 were comparable among homozygous MG53-C14A (ki/ki) and heterozygous MG53-C14A (ki/$^{+}$) mice and their WT littermates in heart and skeletal muscle (Fig. 5*D*).

Although there was no genotype-dependent difference in terms of body weight or basal glucose metabolism, there was a clear beneficial effect from the MG53-C14A mutation when mice were subjected to HFD beginning from 4 weeks of age (Fig. 5*E–H* and Supplementary Fig. 6). In as short as 7 weeks, HFD increased both fasted and fed basal glucose levels in WT mice, but not in MG53-C14A (ki/ki) mice (Fig. 5*F*). With prolonged dietary intervention, HFD led to progressive obesity (Fig. 5*E*), glucose intolerance (Fig. 5*G*), and insulin resistance (Fig. 5*H*). The MG53-C14A mutation effectively ameliorated HFD-induced obesity (Fig. 5*E*) and defects in glucose metabolism (Fig. 5*G* and *H*). Likewise, MG53-C14A (ki/ki) protected the mice against HFD-induced increases in nonesterified fatty acid, triglyceride levels, and body fat/lean ratios (Fig. 6*A–C*); markedly reduced lipid accumulation in multiple organs, including liver and white adipose tissue; and attenuated HFD-induced enlargement of pancreatic islets, without altering the morphology of skeletal muscle, compared with WT littermates (Fig. 6*D*). The beneficial effects of the mutation on metabolic homeostasis were further manifested by attenuated declines in O_2 consumption and energy expenditure after HFD feeding for 32 weeks, with comparable food and drink intake in the knock-in mice (Supplementary Fig. 7*A–C*). Notably, HFD-induced systolic dysfunction of the heart was significantly ameliorated in MG53-C14A (ki/ki) mice, as evidenced by preserved ventricular ejection fraction and left ventricular fractional shortening (Fig. 6*E–G*). As a result, MG53-C14A (ki/ki) mice displayed markedly improved survival profiles relative to WT littermates in response to long-term dietary intervention (Fig. 6*H*). In addition, the protection against cardiac I/R injury in *db/db* mice and the prevention of HFD-induced metabolic disorders in MG53-C14A (ki/ki) mice were also confirmed in female animals (Supplementary Fig. 8*A–F*). These results highlight the high potential of using rhMG53-C14A to treat diet-induced hyperglycemia, dyslipidemia, myocardial injury, and obesity, among other disorders, underscoring an appealing therapeutic strategy, particularly for diabetes-associated myocardial infarction and I/R injury.

Intrinsic IPC Cardioprotection and Tolerance of I/R Injury Remain Intact in MG53-C14A Knock-in Mice

Our previous studies have demonstrated that MG53-deficient hearts are more vulnerable to I/R injury and resistant to IPC protection (17). To investigate the potential impact of the MG53-C14A gene knock-in on intrinsic cardioprotection in mice, we examined I/R-induced myocardial injury and cardiomyocyte death, indexed by infarct size and LDH release, respectively, in perfused hearts isolated from MG53-C14A (ki/ki), Mg53 knockout ($Mg53^{-/-}$), or WT mice in the presence or absence of IPC. There was no significant difference between WT and MG53-C14A (ki/ki) hearts in terms of I/R-induced infarct size or LDH release (Fig. 7*A–C*). In contrast, $Mg53^{-/-}$ mice exhibited overtly enlarged infarct size and persistent LDH release (Fig. 7*A–C*). Importantly, IPC was equally powerful in WT and MG53-C14A knock-in mice, but not in $Mg53^{-/-}$ mice, to protect the heart from I/R injury (Fig. 7*B* and *C*). Thus, the intrinsic IPC cardioprotection was unaffected in MG53-C14A (ki/ki) mice, and the response to I/R injury also remained unaltered. Together, these results indicate that MG53 with a C14A mutation retains cardioprotection without causing metabolic toxic effects.

We next sought to delineate the mechanism underlying MG53-C14A–mediated cardioprotection and its beneficial effects on metabolic homeostasis. In line with our previous notion that MG53 mediates IPC-elicited cardioprotection through activating the RISK survival pathway (17), we found that MG53 and its C14A mutant increased

study, the order of the groups is listed as following: WT chow, MG53-C14A (ki/ki) chow, WT HFD, and MG53-C14A (ki/ki) HFD. Body weights during diet intervention for 32 weeks (n = 5, 5, 10, and 7, respectively) (*E*), fasted and fed blood glucose levels after diet intervention for 7 weeks (n = 6 for each group) (*F*), glucose tolerance tests after diet intervention for 8, 15, and 30 weeks (n = 6, 6, 8, and 8, respectively) (*G*), and insulin tolerance tests after diet intervention for 9, 16, and 31 weeks (n = 4, 4, 10, and 7, respectively) (*H*). All data are presented as mean ± SEM. *E–H*: Statistical analysis was conducted by two-way ANOVA with Tukey multiple comparisons test. *E*, *G*, and *H*: *$P < 0.05$, **$P < 0.01$ for WT HFD vs. WT chow; #$P < 0.05$, ##$P < 0.01$ for MG53-C14A (ki/ki) HFD vs. WT HFD. NS, not significant.

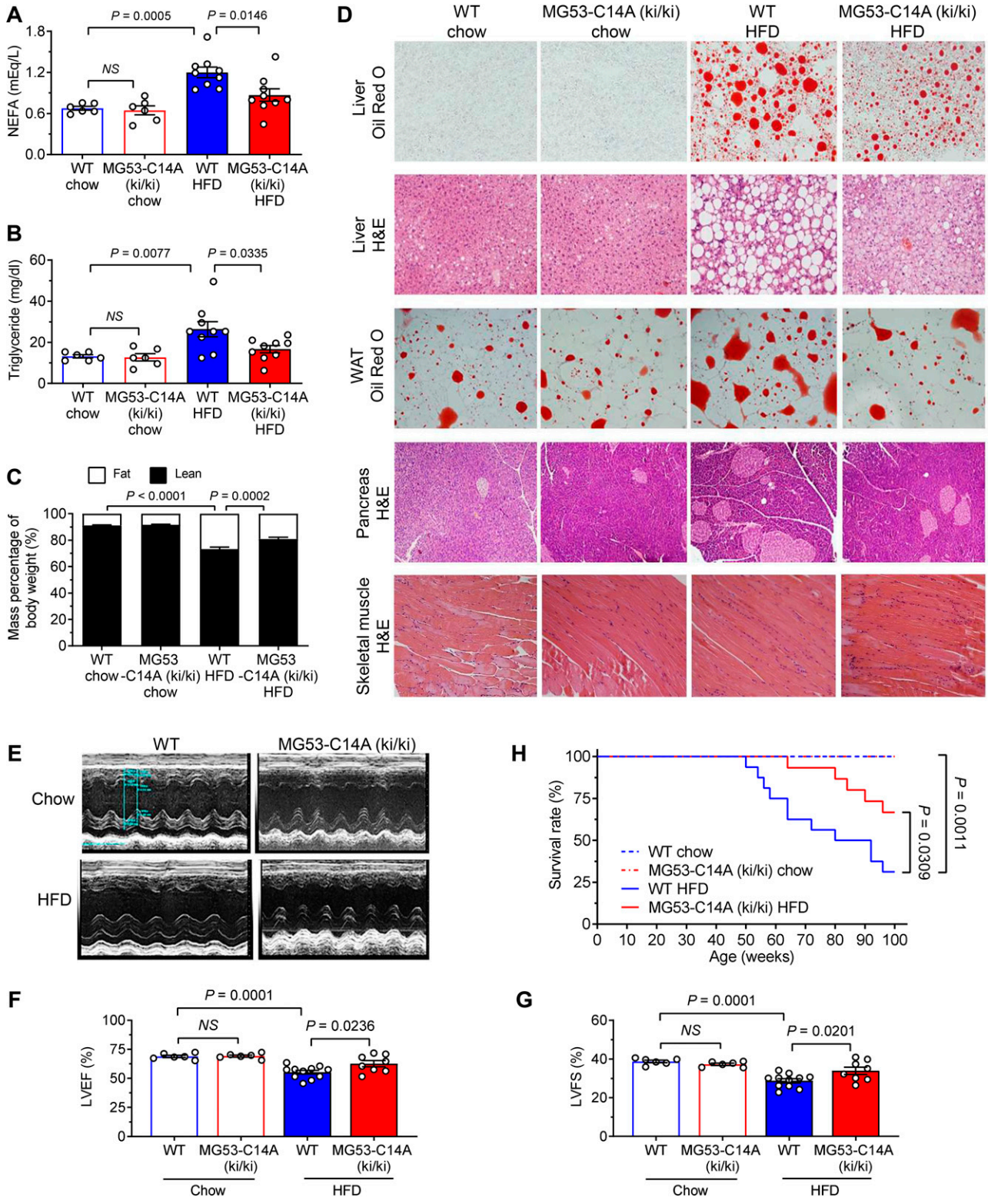

Figure 6—MG53-C14A protects mice from HFD-induced lipid metabolism disorders and cardiac dysfunction. *A–D*: Serum lipid parameters nonesterified fatty acid (NEFA) (*A*) and triglycerides (*B*) after diet intervention for 32 weeks (n = 6 WT chow, n = 6 MG53-C14A [ki/ki] chow, n = 9 WT HFD, and n = 9 MG53-C14A [ki/ki] HFD; the same group order is shown below), mass percentage of body weight detected by magnetic resonance imaging after diet intervention for 8 weeks (n = 4, 6, 7, and 10, respectively; body fat percentages were intercompared here) (*C*), and representative hematoxylin and eosin (H&E) staining of liver, spleen, and skeletal muscle and oil red O staining for liver and white adipose tissue (WAT) after diet intervention for 32 weeks (scale bar 50 μm) (*D*) in WT and MG53-C14A (ki/ki) mice receiving chow or HFD from 4 weeks of age. *E–H*: Representative echocardiography images (*E*), statistical results of left ventricular ejection fraction

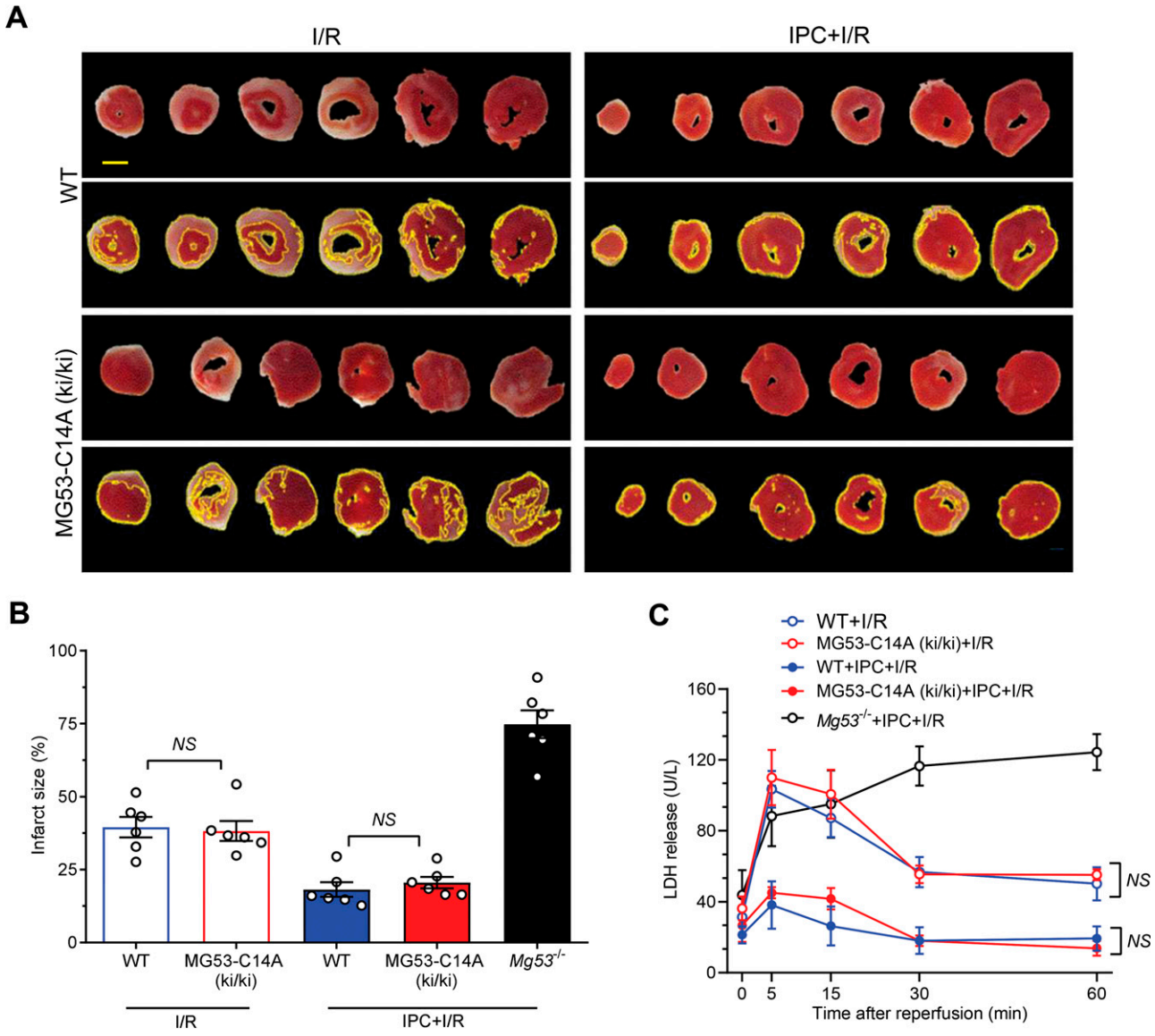

Figure 7—MG53 C14A knock-in mice retain intact cardiac IPC protection against I/R injury. *A–C*: Representative photographs (*A*) and statistical data of infarct size (n = 6) (*B*), and levels of LDH release in effluent (n = 13 WT + I/R, n = 11 MG53-C14A (ki/ki) + I/R, n = 7 WT + IPC + I/R, and n = 6 MG53-C14A (ki/ki) + IPC + I/R) (*C*) of WT and MG53-C14A (ki/ki) of the isolated perfused mouse hearts subjected to I/R ex vivo with or without IPC. *Mg53* knockout ($Mg53^{-/-}$) mice subjected to I/R ex vivo with IPC were positive controls in panel *B* (n = 6 $Mg53^{-/-}$ + IPC + I/R) and panel *C* (n = 4 $Mg53^{-/-}$ + IPC + I/R). Scale bar is 2 mm. All data are presented as mean ± SEM. Statistical analysis was conducted by one-way ANOVA with Tukey multiple comparisons test (*B*) or two-way ANOVA with Tukey multiple comparisons test (*C*). NS, not significant.

phosphorylation of Akt, the central molecular event of the RISK pathway, to a similar extent in cultured cardiomyocytes (Fig. 8*A*), consistent with their equally potent cell protective effects (Fig. 1*E* and *F*). However, in MG53-C14A (ki/ki) mice receiving either chow or HFD, IR and IRS1 protein levels were markedly increased, while their ubiquitination levels were decreased in skeletal muscle (Fig. 8*B–D*), validating MG53-C14A as an E3 ligase–deficient mutant (21). These findings shed new light on our understanding of the beneficial effects of the E3

(LVEF) (*F*) and fractional shortening (LVFS) (*G*) after diet intervention for 32 weeks (n = 6, 6, 11, and 8, respectively), and survival curves (n = 10, 10, 16, and 15, respectively) (*H*) of WT and MG53-C14A (ki/ki) mice receiving chow or HFD from 4 weeks of age. All data are presented as mean ± SEM. Statistical analysis was performed using one-way ANOVA with Tukey multiple comparisons test (*A*, *B*, *F*, and *G*), two-way ANOVA with Tukey multiple comparisons test (*C*), or log-rank (Mantel-Cox) test (*H*). NS, not significant.

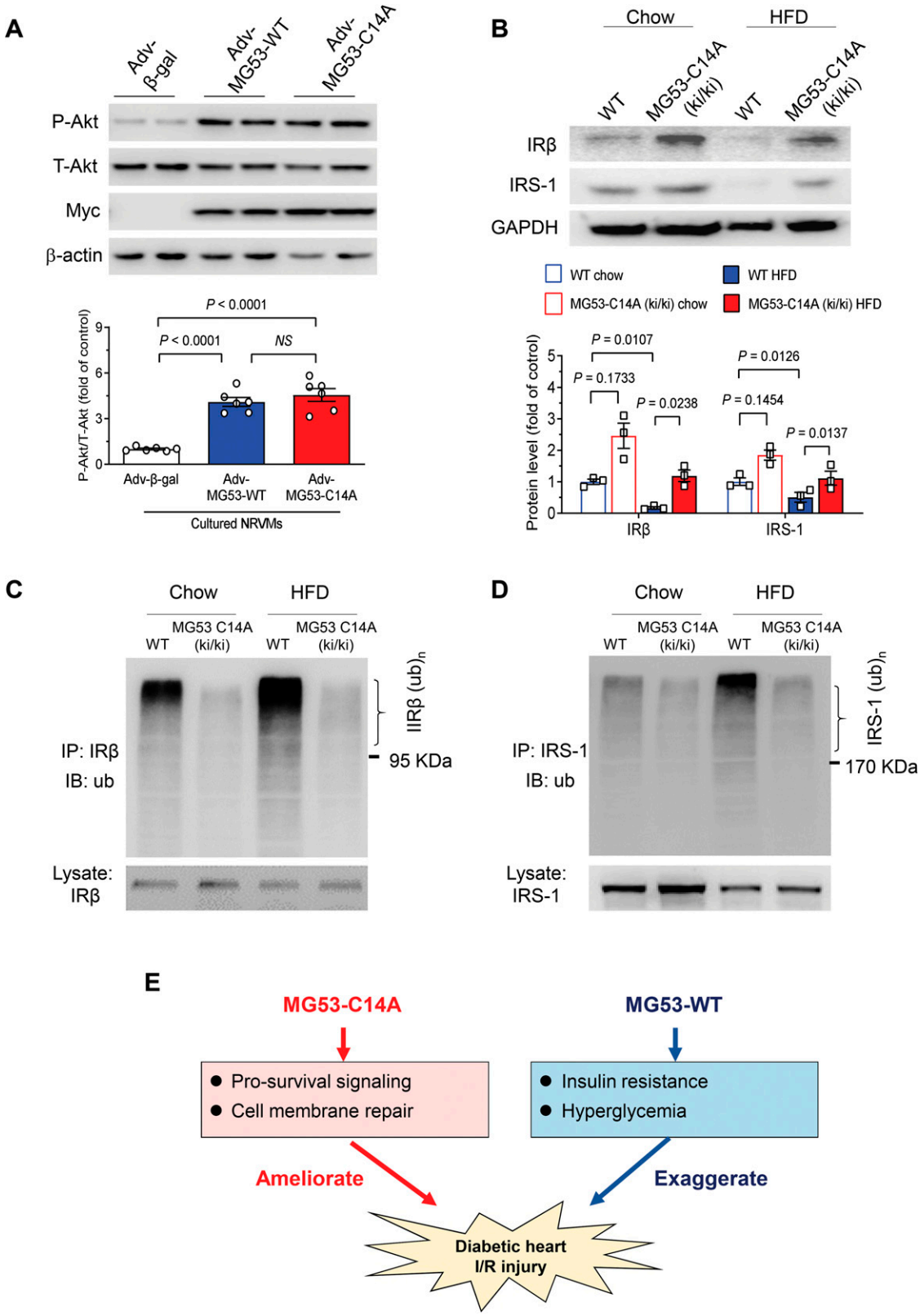

Figure 8—The mechanisms of the cardioprotection and antidiabetic effects of MG53-C14A mutant. *A*: Representative Western blots and statistical analysis of total (T-Akt) and phosphorylated Akt (P-Akt) in cultured rat neonatal cardiomyocytes with adenovirus-mediated overexpression of MG53-WT or MG53-C14A ($n = 6$). Myc served as a marker for adenovirus transfection, and β-actin served as a loading control. *B*: Representative Western blots and statistical analysis of IRβ and IRS1 in the skeletal muscle from WT and MG53-C14A (ki/ki) mice receiving chow diet or HFD at 38 weeks of age ($n = 3$). *C* and *D*: Ubiquitination levels of IRβ (*C*) and IRS1 (*D*) in the skeletal muscle from WT and MG53-C14A (ki/ki) mice receiving chow diet or HFD at 38 weeks of age ($n = 4$). *E*: Schematic diagram showing the role of MG53-WT

ligase–dead mutant MG53-C14A in improving I/R-injured diabetic hearts, in particular, and in preventing HFD-induced metabolic disorders and cardiac defects, in general.

DISCUSSION

Over the past decades, it has been shown that patients with cardiovascular disease in the presence of diabetes experience poorer clinical outcomes (3–7). To develop novel therapy for patients with diabetes with cardiovascular comorbidities, we compared and contrasted the effects of MG53 with those of its E3 ligase–deficient mutant, MG53-C14A, on I/R-injured hearts in normal or diabetic mice. In this study, there are three major findings. First, we have shown that MG53-WT worsens hyperglycemia and I/R-induced cardiac injury and mortality in diabetic mice, although it protects the normal heart against ischemic damage. In contrast, MG53-C14A elicits a profound cardiac protective effect without disrupting metabolic homeostasis in the presence of diabetes. Importantly, using recombinant protein or adenoviral gene transfer approaches, we have demonstrated that prolonged treatment of diabetic mice with MG53-C14A, but not MG53-WT, elicits beneficial effects on the diabetic heart without disrupting metabolic homeostasis (Fig. 4*A*–*K*). Furthermore, the sustained presence of MG53-C14A in the knock-in mice also ameliorated HFD-induced cardiac damage and a cluster of metabolic disorders including obesity, hyperglycemia, and insulin resistance. Thus, MG53-C14A is a promising therapy for the treatment of acute myocardial injury as well as various chronic cardiometabolic diseases, whereas rhMG53-WT is detrimental in the context of diabetes and other metabolic disorders (Fig. 8*E*).

MG53 is a double-edged sword, mediating cardioprotection and metabolic detrimental effects (21–23,32). Mechanistically, as an E3 ligase, MG53 targets IR and IRS1 for ubiquitin-dependent degradation, leading to insulin resistance and hyperglycemia, which raises serious safety concerns for clinical applications of MG53, especially for patients with diabetes and other metabolic diseases. Our previous studies have demonstrated that MG53-C14A is an E3 ligase–dead mutant (21,22,24). In line with this, ubiquitination levels of IR and IRS1 were markedly reduced, leading to increased levels of both proteins in MG53-C14A knock-in mice compared with WT littermates. Importantly, knock-in of MG53-C14A not only retained its cardiac protective effect but also overtly attenuated HFD-induced metabolic disorders, including hyperglycemia, insulin resistance, obesity, organ lipid accumulation, and cardiac dysfunction, marking MG53-C14A mutant as an ideal therapy for the treatment of acute myocardial injury and chronic cardiometabolic disease.

It noteworthy that under the current experimental conditions, a single injection of rMG53-C14A proteins was sufficient to protect the heart from I/R injury, but it had a minor effect on metabolic control in *db*/*db* diabetic and normal mice, while the constant expression of the mutant in the knock-in mice had robust beneficial effects to ameliorate HFD-induced metabolic disorders. Briefly, in *db*/*db* mice, rMG53-C14A was delivered once, and its effects were monitored up to 24 h. Although a single injection of rMG53-C14A had no significant effect on metabolic homeostasis, adenoviral gene transfer–mediated sustained elevation (for ∼1 week) of the mutant protein, in fact, significantly alleviated hyperglycemia and improved insulin sensitivity in *db*/*db* mice (Fig. 4*H* and *I*). Furthermore, in the knock-in mice, the presence of MG53-C14A lasted for >30 weeks, so it had enough time to elicit positive effects on metabolic control against HFD-induced disorders. In addition, daily injection of rhMG53-C14A, instead of rhMG53-WT, for 2 weeks effectively improved the cardiac dysfunction in diabetic *db*/*db* mice. These results provide multiple lines of evidence that the MG53-C14A mutant is a potentially important therapy with an excellent safety profile.

In multiple diabetic mouse models, we have found that acute delivery of MG53-WT does increase blood glucose. In contrast, some previous studies have failed to detect alterations in blood glucose in nondiabetic or diabetic *db*/*db* mice in response to systemic delivery of rhMG53 or adenoviral gene transfer of tissue plasminogen activator MG53 (30,31). The discrepancy between the current and previous studies is, at least in part, attributable to the differences in the basal glucose levels of the animals used. In our study, the fasting blood glucose of all *db*/*db* mice was >10 mmol/L and fed blood glucose was >20 mmol/L at 10 weeks of age, whereas in previous studies, average fasting glucose was ∼7 mmol/L and fed glucose was 13.9 mmol/L for mice at 18–32 weeks of age (30,31). This suggests that the metabolic adverse effects of rhMG53 are only observed in full-blown diabetes.

In this study, the detrimental effect of MG53-WT on diabetic hearts was more prominent pre- compared with posttreatment. Regarding the underlying mechanism, the exaggerated myocardial injury and mortality were accompanied by a more persistent increase in blood glucose, suggesting MG53-induced hyperglycemia not only offsets its cardioprotection, but also aggravates I/R-induced

and MG53-C14A in cardiac I/R injury in diabetic hearts. In diabetic hearts, MG53-WT leads to insulin resistance and hyperglycemia, which not only compromises the efficacy of MG53-mediated cardioprotection, but also exaggerates cardiac I/R injury. In contrast, MG53-C14A effectively ameliorates I/R-induced myocardial injury without eliciting metabolic adverse effects. Data are presented as mean ± SEM. Statistical analysis was conducted by one-way ANOVA with Tukey multiple comparisons test (*A*) or two-way ANOVA with Tukey multiple comparisons test (*B*). IB, immunoblotting; IP, immunoprecipitation; NS, not significant.

damage to the diabetic heart. Under basal conditions, the diabetic heart uses free fatty acid as the major substrate for energy metabolism, but oxidative phosphorylation of free fatty acid could be markedly inhibited because of the lack of O_2 during ischemia. Suppression of glucose use by pre-rhMG53-WT would be expected to increase blood glucose and impair cardiomyocyte glycolysis, thus further reducing cellular energy production and exacerbating ischemic cardiac damage. Therefore, it is reasonable to postulate that circulating MG53 is the prime culprit of abnormal fluctuations in hyperglycemia, and in turn, this metabolic adverse effect would rule out the use of rhMG53-WT for the treatment of myocardial injury because of the safety concerns in individuals with diabetes. Nevertheless, some remaining questions merit future investigation. For instance, it is presently unclear why and how hyperglycemia exaggerates ischemic myocardial injury. Second, posttreatment rather than pretreatment with rhMG53-C14A potently protects the diabetic heart, but the underlying mechanism is not fully understood. Finally, additional preclinical studies in large animal models, such as swine and nonhuman primates, are required to translate rhMG53-C14A into a novel therapy for patients with diabetes.

In summary, in this study, we made three novel findings: *1*) administration of rhMG53-WT is harmful to individuals with diabetes, because it aggravates metabolic disorders and worsens I/R-induced myocardial injury and mortality in mice; *2*) systemic delivery of rhMG53-C14A mutant protein markedly ameliorates cardiac I/R injury without causing metabolic toxic effects; and *3*) chronic expression of MG53-C14A in knock-in mice does not affect cardiac integrity or IPC protection; indeed, it protects mice from HFD-induced metabolic disorders and effectively reduces diet-induced morphologic and functional defects in the heart. These findings define MG53-C14A mutant protein as a potentially important novel therapy for a variety of acute myocardial injuries, as well as a range of chronic cardiometabolic diseases.

Acknowledgments. The authors thank Drs. H.P. Cheng for insightful discussions and H. Shang, W. Zheng, W.Q. Zhang, and X.T. Sun for excellent technical support. The authors also thank Drs. H. Takeshima and J.J. Ma for providing the *Mg53*$^{-/-}$ mice.

Funding. This work was supported by the National Key R&D Program of China (2018YFA0507603, 2018YFA0800701, and 2018YFA0800501) and the National Natural Science Foundation of China (31671177, 81630008, 81790621, 31970722, and 31521062).

Duality of Interest. No potential conflicts of interest relevant to this article were reported.

Author Contributions. H.F., H.S., Y.Z., and R.-P.X. proposed the hypothesis, generated the initial idea, conducted key experiments, and wrote the manuscript. Y.Z. and R.-P.X. designed the study, supervised the experiments and data analysis, wrote the manuscript, and interpreted the results. M.J.R., Y.-H.W., H.-K.W., F.L., and X.H. researched data and contributed to discussion. G.-J.C., S.Z., P.X., L.J., Y.H., and Y.W. researched data. Y.Z. is the guarantor of this work and, as such, had full access to all the data in the study and takes responsibility for the integrity of the data and the accuracy of the data analysis.

References

1. Sattar N, Gill JMR, Alazawi W. Improving prevention strategies for cardiometabolic disease. Nat Med 2020;26:320–325
2. Ezzati M, Riboli E. Can noncommunicable diseases be prevented? Lessons from studies of populations and individuals. Science 2012;337:1482–1487
3. Hammoud T, Tanguay JF, Bourassa MG. Management of coronary artery disease: therapeutic options in patients with diabetes. J Am Coll Cardiol 2000;36:355–365
4. Donahoe SM, Stewart GC, McCabe CH, et al. Diabetes and mortality following acute coronary syndromes. JAMA 2007;298:765–775
5. Flaherty JD, Davidson CJ. Diabetes and coronary revascularization. JAMA 2005;293:1501–1508
6. Berry C, Tardif JC, Bourassa MG. Coronary heart disease in patients with diabetes: part II: recent advances in coronary revascularization. J Am Coll Cardiol 2007;49:643–656
7. Low Wang CC, Hess CN, Hiatt WR, Goldfine AB. Clinical update: cardiovascular disease in diabetes mellitus: atherosclerotic cardiovascular disease and heart failure in type 2 diabetes mellitus - mechanisms, management, and clinical considerations. Circulation 2016;133:2459–2502
8. Kersten JR, Toller WG, Gross ER, Pagel PS, Warltier DC. Diabetes abolishes ischemic preconditioning: role of glucose, insulin, and osmolality. Am J Physiol Heart Circ Physiol 2000;278:H1218–H1224
9. Kristiansen SB, Løfgren B, Støttrup NB, et al. Ischaemic preconditioning does not protect the heart in obese and lean animal models of type 2 diabetes. Diabetologia 2004;47:1716–1721
10. Tsang A, Hausenloy DJ, Mocanu MM, Carr RD, Yellon DM. Preconditioning the diabetic heart: the importance of Akt phosphorylation. Diabetes 2005;54:2360–2364
11. Penna C, Andreadou I, Aragno M, et al. Effect of hyperglycaemia and diabetes on acute myocardial ischaemia-reperfusion injury and cardioprotection by ischaemic conditioning protocols. Br J Pharmacol 2020;177:5312–5335
12. Ferdinandy P, Hausenloy DJ, Heusch G, Baxter GF, Schulz R. Interaction of risk factors, comorbidities, and comedications with ischemia/reperfusion injury and cardioprotection by preconditioning, postconditioning, and remote conditioning. Pharmacol Rev 2014;66:1142–1174
13. Ritsinger V, Malmberg K, Mårtensson A, Rydén L, Wedel H, Norhammar A. Intensified insulin-based glycaemic control after myocardial infarction: mortality during 20 year follow-up of the randomised Diabetes Mellitus Insulin Glucose Infusion in Acute Myocardial Infarction (DIGAMI 1) trial. Lancet Diabetes Endocrinol 2014;2:627–633
14. Capes SE, Hunt D, Malmberg K, Gerstein HC. Stress hyperglycaemia and increased risk of death after myocardial infarction in patients with and without diabetes: a systematic overview. Lancet 2000;355:773–778
15. Huang JP, Huang SS, Deng JY, Hung LM. Impairment of insulin-stimulated Akt/GLUT4 signaling is associated with cardiac contractile dysfunction and aggravates I/R injury in STZ-diabetic rats. J Biomed Sci 2009;16:77
16. Arnold SV, Bhatt DL, Barsness GW, et al.; American Heart Association Council on Lifestyle and Cardiometabolic Health and Council on Clinical Cardiology. Clinical management of stable coronary artery disease in patients with type 2 diabetes mellitus: a scientific statement from the American Heart Association. Circulation 2020;141:e779–e806
17. Cao CM, Zhang Y, Weisleder N, et al. MG53 constitutes a primary determinant of cardiac ischemic preconditioning. Circulation 2010;121:2565–2574
18. Zhang Y, Lv F, Jin L, et al. MG53 participates in ischaemic postconditioning through the RISK signalling pathway. Cardiovasc Res 2011;91:108–115

19. Shan D, Guo S, Wu HK, et al. Cardiac ischemic preconditioning promotes MG53 secretion through H2O2-activated protein kinase C-δ signaling. Circulation 2020;142:1077–1091
20. Liu J, Zhu H, Zheng Y, et al. Cardioprotection of recombinant human MG53 protein in a porcine model of ischemia and reperfusion injury. J Mol Cell Cardiol 2015;80:10–19
21. Song R, Peng W, Zhang Y, et al. Central role of E3 ubiquitin ligase MG53 in insulin resistance and metabolic disorders. Nature 2013;494:375–379
22. Yi JS, Park JS, Ham YM, et al. MG53-induced IRS-1 ubiquitination negatively regulates skeletal myogenesis and insulin signalling. Nat Commun 2013;4:2354
23. Wu HK, Zhang Y, Cao CM, et al. Glucose-sensitive myokine/cardiokine MG53 regulates systemic insulin response and metabolic homeostasis. Circulation 2019;139:901–914
24. Lee H, Park JJ, Nguyen N, et al. MG53-IRS-1 (mitsugumin 53-insulin receptor substrate-1) interaction disruptor sensitizes insulin signaling in skeletal muscle. J Biol Chem 2016;291:26627–26635
25. Lindsey ML, Bolli R, Canty JM Jr, et al. Guidelines for experimental models of myocardial ischemia and infarction. Am J Physiol Heart Circ Physiol 2018;314:H812–H838
26. Bøtker HE, Hausenloy D, Andreadou I, et al. Practical guidelines for rigor and reproducibility in preclinical and clinical studies on cardioprotection. Basic Res Cardiol 2018;113:39
27. Xiao CY, Hara A, Yuhki K, et al. Roles of prostaglandin I(2) and thromboxane A(2) in cardiac ischemia-reperfusion injury: a study using mice lacking their respective receptors. Circulation 2001;104:2210–2215
28. Sui J, Bai J, St Clair Tallarico A, Xu C, Marasco WA. Identification of CD4 and transferrin receptor antibodies by CXCR4 antibody-guided Pathfinder selection. Eur J Biochem 2003;270:4497–4506
29. Lemckert FA, Bournazos A, Eckert DM, et al. Lack of MG53 in human heart precludes utility as a biomarker of myocardial injury or endogenous cardioprotective factor. Cardiovasc Res 2016;110:178–187
30. Wang Q, Bian Z, Jiang Q, et al. MG53 does not manifest the development of diabetes in db/db mice. Diabetes 2020;69:1052–1064
31. Bian Z, Wang Q, Zhou X, et al. Sustained elevation of MG53 in the bloodstream increases tissue regenerative capacity without compromising metabolic function. Nat Commun 2019;10:4659
32. Liu F, Song R, Feng Y, et al. Upregulation of MG53 induces diabetic cardiomyopathy through transcriptional activation of peroxisome proliferation-activated receptor α. Circulation 2015;131:795–804